Novel Quantum Phases of Dipolar Bose Gases in Optical Lattices

S. Yi,[1] T. Li,[2] and C. P. Sun[1]

[1]*Institute of Theoretical Physics, Chinese Academy of Sciences, Beijing, 100080, People's Republic of China*
[2]*Department of Physics, Renmin University of China, Beijing, 100872, People's Republic of China*

(Received 1 January 2007; published 28 June 2007)

We investigate the quantum phases of polarized dipolar bosons loaded into a two-dimensional square and three-dimensional cubic optical lattices. We show that the long-range and anisotropic nature of the dipole-dipole interaction induces a rich variety of quantum phases, including the supersolid and striped supersolid phases in two-dimensional lattices, and the layered supersolid phase in three-dimensional lattices.

DOI: 10.1103/PhysRevLett.98.260405 PACS numbers: 05.30.Jp, 03.75.Lm, 64.60.Cn

The theoretical prediction [1] and experimental realization [2] of the superfluid (SF) to Mott insulating (MI) transition in an atomic system have triggered tremendous research activities on ultracold atoms in an optical lattice. The physics of atomic gases in an optical lattice is captured by the on-site Bose-Hubbard model [1]; however, it has the limitation of lacking off site density-density correlation, which is essential for the emergence of density wave (DW) order and more intriguingly the supersolid (SS) phase [3–7]. Recently, it was proposed that the off site density-density couplings can be realized by the bosons in higher bands of optical lattices [7], by interaction mediated through fermions in a mixture of bosonic and fermionic atoms [8], and, more directly, by the long-range dipole-dipole interaction between dipolar bosons [5]. Among these, dipolar interaction has the advantage of high tunability and experimental accessibility, especially with the recently achieved chromium condensate [9] and ultracold polar molecules in a three-dimensional (3D) optical lattice [10]. So far, ultracold dipolar Bose gases have attracted significant theoretical interest, for the dipole-dipole interaction gives rise to new phenomena in Bose-Einstein condensates [11–14] and provides new schemes for quantum computing [15]. In particular, when loaded into optical lattice potential, the dipolar interaction may induce exotic magnetic orders if the dipole moments are free to rotate in space [16].

In this Letter, we map out the phase diagrams of polarized dipolar bosons in two-dimensional (2D) square and 3D cubic optical lattices. For a 2D lattice on the xy plane, the dipole moments may point either to the z or the y axis; the former corresponds to a 2D isotropic model as the dipolar interaction is isotropic on the lattice plane, while the latter is referred to as the 2D anisotropic model for the anisotropic dipolar interaction on the xy plane. For 3D lattices, we always assume that the dipole moments point to the z direction. As we shall show below, the long-range and anisotropic nature of the dipolar interaction give rise to extremely rich quantum phases. In addition to the SS and checkerboard phases found in Ref. [5], we also predict the striped supersolid (SSS) phases in 2D anisotropic model, and, more remarkably, the layered supersolid (LSS) phase in 3D lattices.

In the presence of dipole-dipole interaction, the Hamiltonian for the extended Bose-Hubbard model reads [5]

$$H = -t\sum_{\langle i,j\rangle}(b_i^\dagger b_j + b_j^\dagger b_i) - \mu\sum_i n_i + \frac{U_0}{2}\sum_i n_i(n_i-1) + \frac{1}{2}\sum_i U_{\mathrm{dd}}^{ii} n_i(n_i-1) + \frac{1}{2}\sum_{i\neq j} U_{\mathrm{dd}}^{ij} n_i n_j, \quad (1)$$

where $b_i^\dagger$ is the boson creation operator at site i and $n_i = b_i^\dagger b_i$ is the corresponding particle number operator. t is the hopping matrix element between nearest neighbors, $U_0 > 0$ is the on site Hubbard repulsion due to s-wave scattering, and, throughout this Letter, the chemical potential μ is fixed at $0.4U_0$.

The last line of Eq. (1) describes the dipolar interaction with coupling parameters being expressed as $U_{\mathrm{dd}}^{ij} = f c_{\mathrm{dd}} \mathcal{D}_{ij}$, where f is a factor continuously tunable between $-\frac{1}{2}$ and 1 via a fast rotating orienting field [17]. As we shall show below, nontrivial quantum phases appear for negative f values. $c_{\mathrm{dd}} = d^2/(4\pi\varepsilon_0)$ or $\mu_0 d^2/(4\pi)$ for, respectively, the electric or magnetic dipoles, with d being the dipole moment and ε_0 (μ_0) being the vacuum permittivity (permeability).

$$\mathcal{D}_{ij} = \int d\mathbf{r} d\mathbf{r}' |w(\mathbf{r}-\mathbf{r}_i)|^2 \frac{1-3\cos^2\theta}{|\mathbf{r}-\mathbf{r}'|^3} |w(\mathbf{r}'-\mathbf{r}_j)|^2, \quad (2)$$

where $w(\mathbf{r}-\mathbf{r}_i)$ is the localized (on site i) Wannier function of the lowest energy band and θ is the angle formed by the dipole moment and the vector $(\mathbf{r}-\mathbf{r}')$. Since $\mathcal{D}_{ij}$ only depends on $\mathbf{r}_i - \mathbf{r}_j = a(l_x\hat{\mathbf{x}} + l_y\hat{\mathbf{y}} + l_z\hat{\mathbf{z}})$ with a being lattice constant and $l_{x,y,z}$ being integers, it can be equivalently denoted as $\mathcal{D}_{(l_x l_y l_z)}$.

In principle, t, U_0, and $\{U_{\mathrm{dd}}^{ij}\}$ are all determined by the optical lattice parameters [5]. However, to obtain a complete phase diagram, we shall allow them to change inde-

pendently except that the set of $\{U_{\rm dd}^{ij}\}$ has to be calculated consistently for a given lattice geometry. For simplicity, we calculate $\mathcal{D}_{(l_x l_y l_z)}$ using a spherical Gaussian function of width σ, $w(\mathbf{r}-\mathbf{r}_i)=\pi^{-3/4}\sigma^{-3/2}e^{-(\mathbf{r}-\mathbf{r}_i)^2/(2\sigma^2)}$, for which $\mathcal{D}_{(000)}$ vanish [18]. All results presented in this work are obtained with $\mathcal{D}_{(l_x l_y l_z)}$ corresponding to $(\sigma, a)=(1,3)$. Similar numerical results are found with other (σ, a) combinations. For practical purposes, we choose to truncate $l_{x,y,z}$ according to $-l_{\max}\le l_{x,y,z}\le l_{\max}$ with $l_{\max}=2$. We have also performed simulations using $l_{\max}$ up to 6 and 3 for, respectively, 2D and 3D lattices, which yield similar qualitative pictures.

To simplify the notation, we define a dimensionless parameter $\gamma\equiv f c_{\rm dd}(4\pi\hbar^2 a_{\rm sc}/M)^{-1}$ to measure the relative strength of dipolar interaction, where $a_{\rm sc}$ is the s-wave scattering length and M is the mass of the atom. It can be easily estimated that $\gamma\approx 0.033f$ for a ^{52}Cr atom and $\gamma\approx 5.68f$ for a typical polar molecule [19]. Finally, the mean-field ground state of Hamiltonian (1) is obtained using Gutzwiller ansatz [1,5] on lattices up to 96×96 and $24\times 24\times 24$ sites with periodic boundary conditions. The Gutzwiller ansatz has been widely used to study the ground state and the dynamics of cold bosons in optical lattices [1,5,12], as it can capture qualitatively the quantum phases, especially in 3D lattices [20].

2D isotropic model.—As shown in Fig. 1, only MI and SF phases appear when γ is negative, which is similar to the on site Bose-Hubbard model with $|\gamma|$ playing effectively the role of the chemical potential. The boundary between two adjacent MI phases is a horizontal line, whose position can be determined analytically as follows: the energy per site for an MI phase is

$$\mathcal{E}/U_0=\rho(\rho-1)/2-\mu\rho/U_0+\gamma\varepsilon_{\rm dd}\rho^2, \qquad (3)$$

where ρ is the mean particle density and $\gamma\varepsilon_{\rm dd}$ is the dipolar interaction energy per site for the MI-1 phase. The boundary between MI-ρ and MI-$(\rho+1)$ phases is then located at $\gamma=(\mu/U_0-\rho)/[\varepsilon_{\rm dd}(2\rho+1)]$. Furthermore, a MI phase is stable only if $\gamma\varepsilon_{\rm dd}+1/2>0$; hence, the system collapses for $\gamma\lesssim -0.41$, in very good agreement with our numerical result. This stability criterion also applies roughly to the SF phase.

For positive γ, the SS and DW phases emerge in addition to the usual SF and MI phases. In particular, the large lobe denoted as DW-1/2 corresponds to the checkerboard phase, where sites are alternatingly empty and singly occupied. We note that the checkerboard and SF phases are not connected directly, in accord with the Landau theory of phase transition; namely, phases with distinct symmetry breaking patterns cannot be connected with each other continuously. Both DW-h and -l regions contain many small DW lobes with different mean densities, as these DW lobes are very sensitive to t, γ, and the size of lattice, it is very difficult to map them out in detail.

From the above discussions, it is clear that the repulsive dipolar interaction ($\gamma>0$) with sufficient strength breaks the translational symmetry, while the attractive one ($\gamma<0$) always preserves it. The symmetry breaking and preserving property of the dipolar interactions can be understood intuitively as follows: supposing that site i is occupied, it is energetically favorable that its neighboring sites are equally (less) populated if the dipole-dipole interaction is attractive (repulsive).

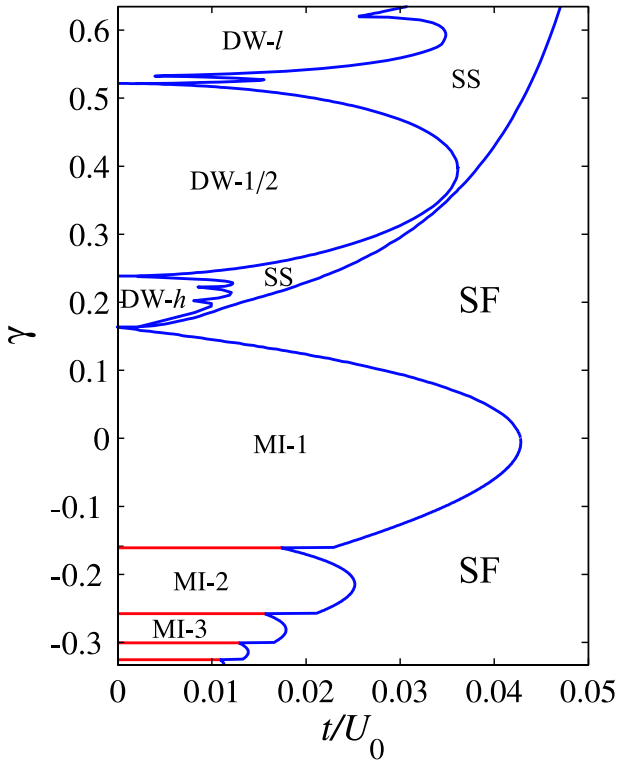

FIG. 1 (color online). Phase diagram in t-γ parameter plane for 2D isotropic model obtained on a 12×12 lattice. Various MI-ρ phases are distinguished by the occupation number ρ. DW-1/2 denotes the checkerboard phase. In DW-h (DW-l) region, there exist many small DW lobes with the mean densities higher (lower) than 1/2. The phase transitions between various insulating phases are of first order, while all other transitions are of second order. This observation also applies to Figs. 2 and 4(a).

2D anisotropic model.—As dipole moments are polarized along the y axis, the dipolar interaction along the y (x) direction is attractive (repulsive) for positive γ, while for negative γ the opposite is true. Based on the relation between dipolar interaction and translational symmetry, we expect to find stripe ordering here. The phase diagram presented in Fig. 2 indeed confirms our conjecture. Considering, for example, the insulating phases in Fig. 2, the particle density along the repulsive direction becomes periodically modulated for sufficiently large $|\gamma|$, while it remains to be a constant along the attractive direction. The structure of a striped insulating phase is then completely specified by the particle densities over a single modulation period as $[\rho_1,\rho_2,\ldots,\rho_m]$.

There exists a subtle difference between the dipolar interactions corresponding to negative and positive γ: for

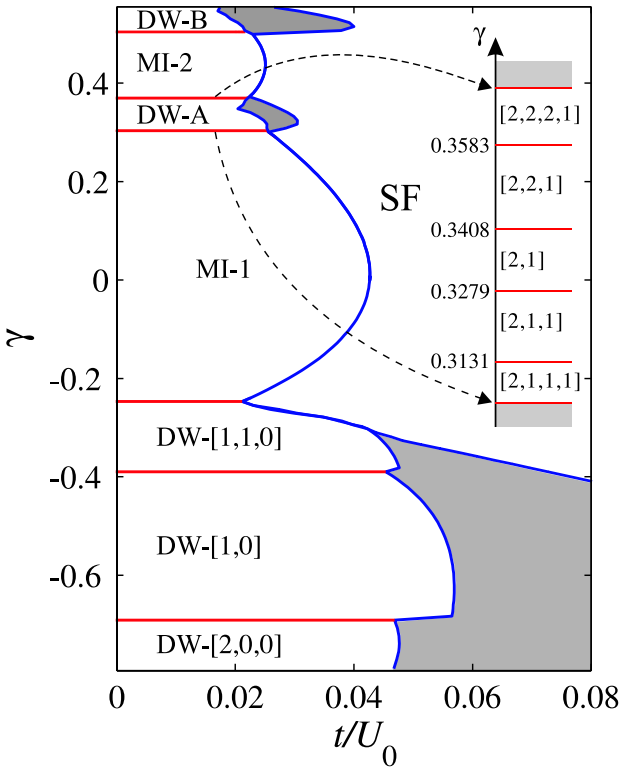

FIG. 2 (color online). Same as Fig. 1 except for 2D anisotropic model. The DW phases for $\gamma < 0$ are distinguished by their density distributions. For $\gamma > 0$, both DW-A and -B regions contain fine structures. The shaded regions represent the SSS phases. The inset shows the zoom-in plot of DW-A region. DW-B has a similar structure except that the occupation number on each site is increased by 1.

a uniform density distribution, the overall dipolar interaction is attractive (repulsive) for the positive (negative) γ. Consequently, as the dipolar coupling grows, the mean density generally increases for positive γ, while it decreases for negative γ. The DW-$[2, 0, 0]$ phase, on the other hand, has higher mean density compared to DW-$[1, 0]$, for this configuration results in a lower dipolar interaction energy. As we further increase $|\gamma|$, the system collapses for roughly $\gamma \gtrsim 0.63$ and $\gamma \lesssim -1.27$. More interestingly, the shaded regions, to the right of the striped solid phases, represent the SSS phase with a density distribution resembling their insulting counterparts. Recently, the stripe ordered SS phase was also predicted in the p-band Bose-Hubbard model of 2D triangular lattices [21].

To gain more insight into the stripe ordering, we reexamine the Hamilton (1) in the hard-core limit, where it maps onto a spin-$\frac{1}{2}$ XXZ model

$$H = -t\sum_{\langle i,j\rangle}(s_i^+ s_j^- + \text{H.c.}) + \frac{1}{2}\sum_{i\neq j} U_{dd}^{ij} s_i^z s_j^z - h_z \sum_i s_i^z \quad (4)$$

with $h_z = \mu - \gamma\epsilon_{\text{dd}}/2$. Here the ferromagnetic ordering in the xy plane corresponds to the superfluidity in Eq. (1), and the modulation in s_i^z corresponds to the ordering of the density. For simplicity, we only take into account the dipolar interaction between nearest neighboring (NN) sites. Figure 3 shows the phase diagram obtained through numerical optimization. Compared to Fig. 2, the SSS regions here are rather small. Since inclusion of the next-nearest-neighboring (NNN) coupling does not help much, we conclude that the soft-core nature of Eq. (1) should be responsible for the large stable SSS phases in Fig. 2. This also explains the absence of SSS phase for $f > 0$. For the isotropic model, NNN coupling is the key factor for the presence of SSS phase. It not only provides frustration necessary for SS order, but it is also responsible for the stripe ordering at large NNN coupling strength [22]. Here, however, due to the anisotropic nature of the long-range interaction, the NN coupling alone is sufficient for generating the SSS phase.

3D lattices.—In Fig. 4(a), we plot the phase diagram for dipolar bosons in a 3D lattice. A special feature we note immediately is that the right boundary of the MI-1 phase is a vertical line. This is because our cutoff scheme on $l_{x,y,z}$ makes the dipolar interaction energy vanish for a uniform density distribution on a 3D cubic lattice. For positive γ, the dipolar interaction is repulsive on the lattice planes perpendicular to the z axis; therefore, DW order emerges on each lattice layer for sufficiently large γ, in analogy to the 2D isotropic model. However, as the dipolar interaction is attractive along the z axis, the density distributions on different lattice layers are identical. The detailed structure of the DW-C region is rather complicated. In general, the mean density first decreases with γ, then increases slightly until the system collapses at $\gamma \approx 0.63$. The SS phase has a similar density structure to that of the DW-C phase.

For negative γ, one can naturally expect the layered phases due to the attractive dipolar interaction on the lattice layer. In other words, for a layered phase, the particle density within each layer is a constant while periodically modulated along the z axis. In Fig. 4(a), the layered insulating phases are specified by the densities on lattice layers

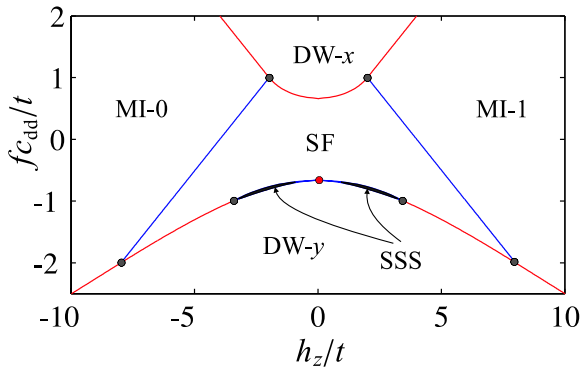

FIG. 3 (color online). Mean-field phase diagram for spin-$\frac{1}{2}$ model Eq. (4) with nearest neighbor coupling. In MI-0 phase, lattice sites are not occupied. DW-x (DW-y) denotes the striped solid phase with density modulation along x (y) direction. The shaded regions represent the SSS phases.

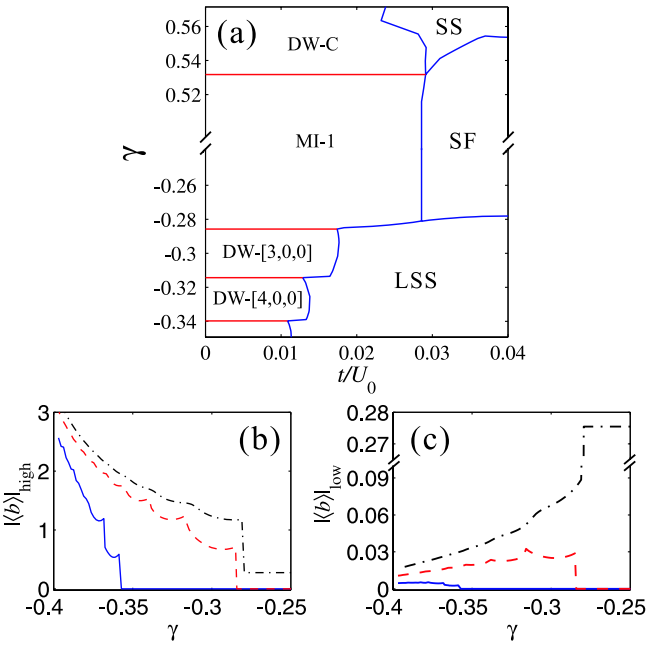

FIG. 4 (color online). (a) Mean-field phase diagram for dipolar bosons in 3D cubic lattice obtained on a $6 \times 6 \times 6$ lattice. The lower panels show the γ dependence of superfluid parameters on high (b) and low (c) density layers for $t/U_0 = 0.01$ (solid lines), 0.02 (dashed lines), and 0.03 (dash-dotted lines).

over a single modulation period. Unlike the 2D case, the only density modulation period we found is 3 even for a lattice whose size is not a multiple of 3. Same as the 2D isotropic case, the onset of instability occurs at $\gamma \approx -0.41$.

The structure of the LSS phase is similar to that of a layered solid phase: each modulation period contains a layer with higher density and two layers with equal lower densities. Figures 4(b) and 4(c) show the γ dependence of the SF order parameter $|\langle b \rangle|$ on, respectively, the high and low density layers. In general, the SF parameter increases with $|\gamma|$ on high density layers, while it decreases on low density layers. In the strong dipolar interaction limit, $|\langle b \rangle|_{\text{high}}$ can be 2 orders of magnitude larger than $|\langle b \rangle|_{\text{low}}$. If we treat the low density layers as a charge reservoir unit, then the resulting structure is quite similar to that of a high-T_c cuprate superconductor.

In conclusion, we have studied the quantum phases of dipolar bosons in optical lattice. We have shown that, due to the long-range and anisotropic nature of dipole-dipole interaction and its tunability, the achievable phases in this system are extremely rich, which makes dipolar bosons in a lattice an ideal candidate for studying the exotic phases in a strongly correlated quantum system. The experimental detection of SSS and LSS phases in chromium atoms relies on tuning the scattering length to below 10 bohr radius, while they should be observable in typical polar molecule systems.

This work is supported by the NSFC and the National Programme for Fundamental Research of China. S. Y. is also supported by the "BaiRen" program of CAS. We thank H. Pu for a critical reading of the manuscript. The helpful discussions with Jinwu Ye and the correspondence with L. Santos on numerical calculation are acknowledged.

[1] D. Jaksch *et al.*, Phys. Rev. Lett. **81**, 3108 (1998).
[2] M. Greiner *et al.*, Nature (London) **415**, 39 (2002).
[3] O. Penrose and L. Onsager, Phys. Rev. **104**, 576 (1956).
[4] E. Kim and M. H. W. Chan, Nature (London) **427**, 225 (2004); Science **305**, 1941 (2004).
[5] K. Góral, L. Santos, and M. Lewenstein, Phys. Rev. Lett. **88**, 170406 (2002).
[6] M. Boninsegni and N. Prokof'ev, Phys. Rev. Lett. **95**, 237204 (2005); S. Wessel and M. Troyer, *ibid.* **95**, 127205 (2005); D. Heidarian and K. Damle, *ibid.* **95**, 127206 (2005); R. G. Melko *et al.*, *ibid.* **95**, 127207 (2005).
[7] V. W. Scarola and S. Das Sarma, Phys. Rev. Lett. **95**, 033003 (2005).
[8] H. P. Büchler and G. Blatter, Phys. Rev. Lett. **91**, 130404 (2003).
[9] A. Griesmaier *et al.*, Phys. Rev. Lett. **94**, 160401 (2005).
[10] C. Ospelkaus *et al.*, Phys. Rev. Lett. **97**, 120402 (2006).
[11] S. Yi and L. You, Phys. Rev. A **61**, 041604 (2000); K. Góral, K. Rzążewski, and T. Pfau, *ibid.* **61**, 051601 (2000); L. Santos *et al.*, Phys. Rev. Lett. **85**, 1791 (2000).
[12] B. Damski *et al.*, Phys. Rev. Lett. **90**, 110401 (2003).
[13] Z. W. Xie and W. M. Liu, Phys. Rev. A **70**, 045602 (2004).
[14] S. Yi, L. You, and H. Pu, Phys. Rev. Lett. **93**, 040403 (2004); Y. Kawaguchi, H. Saito, and M. Ueda, *ibid.* **96**, 080405 (2006); L. Santos and T. Pfau, *ibid.* **96**, 190404 (2006); S. Yi and H. Pu, *ibid.* **97**, 020401 (2006).
[15] D. DeMille, Phys. Rev. Lett. **88**, 067901 (2002); A. André *et al.*, Nature Phys. **2**, 636 (2006).
[16] H. Pu, W. Zhang, and P. Meystre, Phys. Rev. Lett. **87**, 140405 (2001); R. Barnett *et al.*, Phys. Rev. Lett. **96**, 190401 (2006); A. Micheli, G. K. Brennen, and P. Zoller, Nature Phys. **2**, 341 (2006).
[17] S. Giovanazzi, A. Görlitz, and T. Pfau, Phys. Rev. Lett. **89**, 130401 (2002).
[18] Even for a 2D lattice, the spherically symmetrical $w(\mathbf{r} - \mathbf{r}')$ can still be realized by applying a harmonic trap with appropriate trapping frequency along the z direction.
[19] For chromium atoms, $d = 6\mu_B$ and $a_{sc} = 112a_B$; for typical polar molecules, $d = 0.5$ D, $a_{sc} = 100a_B$, and M is around 100 atomic number.
[20] W. Zwerger, J. Opt. B **5**, S9 (2003).
[21] C.-J. Wu *et al.*, Phys. Rev. Lett. **97**, 190406 (2006).
[22] See, e.g., R. T. Scalettar *et al.*, Phys. Rev. B **51**, 8467 (1995).